



Spin splitting in graphene studied by means of tilted magnetic-field experiments

E. V. Kurganova,^{1,*} H. J. van Elferen,¹ A. McCollam,¹ L. A. Ponomarenko,² K. S. Novoselov,² A. Veligura,³
B. J. van Wees,³ J. C. Maan,¹ and U. Zeitler^{1,†}

¹*High Field Magnet Laboratory, Institute for Molecules and Materials, Radboud University Nijmegen, Toernooiveld 7,
NL-6525 ED Nijmegen, The Netherlands*

²*School of Physics and Astronomy, University of Manchester, M13 9PL, Manchester, United Kingdom*

³*Physics of Nanodevices, Zernike Institute for Advanced Materials, University of Groningen,
Nijenborgh 4, NL-9747 AG Groningen, The Netherlands*

(Received 18 July 2011; revised manuscript received 22 August 2011; published 20 September 2011)

We have measured the spin splitting in single-layer and bilayer graphene by means of tilted magnetic-field experiments. By applying the Lifshitz-Kosevich formula for the spin-induced decrease of the Shubnikov-de Haas amplitudes with increasing tilt angle, we directly determine the product between the carrier cyclotron mass m^* and the effective g factor g^* as a function of the charge-carrier concentration. By using the cyclotron mass for a single-layer and a bilayer graphene, we find an enhanced g factor $g^* = 2.7 \pm 0.2$ for both systems.

DOI: 10.1103/PhysRevB.84.121407

PACS number(s): 72.80.Vp, 71.70.Ej, 71.70.Di

The half-integer quantum Hall effect in single-layer graphene (SLG)^{1,2} and the unconventional quantum Hall effect in bilayer graphene (BLG)³ reveal spin- and valley-degenerate relativistic Landau levels. Due to the extremely large Landau-level splitting,^{4,5} completely resolved levels can be observed up to room temperature.⁶ However, even at very high perpendicular magnetic fields the Zeeman splitting within one Landau level is negligible smaller compared to the Landau-level splitting and, more importantly, the Landau-level width generally exceeds the spin splitting. Exceptionally, the zeroth Landau level in SLG becomes extremely narrow at magnetic fields $B > 20$ T,⁴ which allows an experimental observation of a spin-related gap opening at magnetic fields $B > 20$ T.⁷ Another observation of a spin degeneracy lifting with an effective g factor $g^* = 2$ was reported for $\nu = \pm 4$, in SLG for magnetic fields $B > 30$ T, combined with lifting the valley degeneracy at $\nu = \pm 1$.⁸

In this Rapid Communication we determine the spin splitting of broadened Landau levels for SLG and BLG by measuring Shubnikov-de Haas (SdH) oscillations in tilted magnetic fields. This technique allows adjusting the ratio between the spin splitting and the Landau-level splitting by controlling the ratio between a total magnetic field and a component perpendicular to a two-dimensional graphene flake. Using the well-established Lifshitz-Kosevich formula^{9,10} we determine the product of the effective g factor and cyclotron mass m^*g^* from the angular dependence of the SdH amplitudes and we find that g^* is enhanced compared to the free-electron value.

We have fabricated field-effect transistors from SLG and BLG by micromechanically exfoliating graphene flakes from graphite. The flakes were deposited on top of a Si/SiO₂ wafer, structured into a Hall bar and covered with Au/Ti contacts.¹¹ Charge carriers are introduced by applying a gate voltage on the conducting Si substrate.

We present a detailed analysis on the spin splitting in a SLG sample made from Kish graphite with a mobility $\mu = 0.8$ V m⁻² s⁻¹ and a BLG sample originating from natural graphite with a mobility $\mu = 0.3$ V m⁻² s⁻¹. Two other devices, one SLG and one BLG sample, showed qualitatively similar results.

To determine the spin splitting we have measured the longitudinal resistances R_{xx} as a function of charge-carrier concentration n at a constant perpendicular magnetic field. We adjusted the total magnetic field B_{tot} for each tilt angle such that the normal component B_n is the same (see the inset to Fig. 1). The value of B_n was verified by measuring the Hall resistance of the devices in the nonquantized regime.

In Fig. 1 we show the experimental $R_{xx}(n)$ dependencies for SLG at $B_n = 6$ T (a) and for BLG at $B_n = 8$ T (b). R_{xx} shows Shubnikov-de Haas oscillations with maxima whenever the Fermi energy is situated in the middle of a spin- and valley-degenerated Landau level E_N , $N = 0, 1, 2, \dots$ being the Landau-level index. For the higher Landau levels ($N \geq 2$) the longitudinal resistances do not exhibit zero minima, indicating that the level broadening is comparable to the cyclotron energy at these perpendicular magnetic fields.

When increasing B_{tot} at a constant B_n , the oscillation amplitudes for both BLG and SLG are reduced. From this reduction we determined the spin splitting. We use the Lifshitz-Kosevich formula for systems with a general dispersion and we specifically include spin splitting^{9,10} with an effective g factor g^* (Refs. 12 and 13) and tilted magnetic fields.¹⁴ The oscillatory contribution to the longitudinal resistance can be described as²

$$\tilde{R}_{xx} = A \cos \left(\frac{\hbar}{eB_n} S(E)|_{E=E_F} + \pi + \varphi_B \right), \quad (1)$$

where $S(E)|_{E=E_F}$ is an extremal cross section of the Landau orbits in the k space, A is the oscillation amplitude, and φ_B is the Berry phase, $\varphi_B = \pi$ for SLG,^{1,2} and $\varphi_B = 2\pi$ for BLG.³ The amplitude A contains a monotonic n -dependent part, a temperature dependence, a B_n -dependent contribution, and a damping factor due to spin splitting depending on the total field B_{tot} . At a constant temperature and perpendicular magnetic field this B_{tot} dependence of the SdH amplitude A for charge carriers with cyclotron mass m^* and effective g factor g^* is given by^{12,14}

$$A = A_0(N) \cos \left(\frac{\pi}{2} \frac{g^* m^* B_{\text{tot}}}{m_e B_n} \right), \quad (2)$$

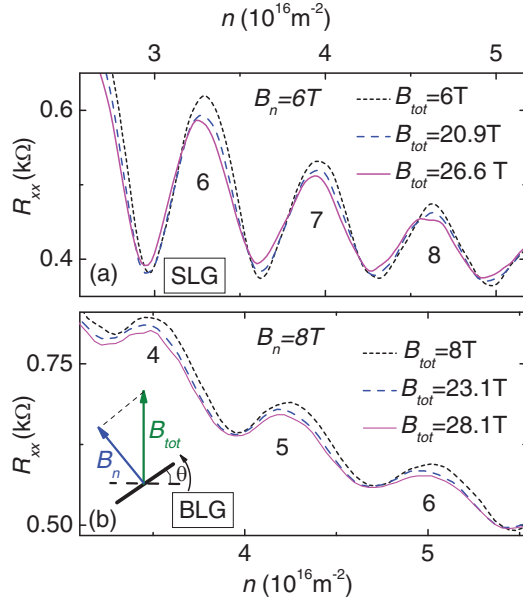


FIG. 1. (Color online) Shubnikov-de Haas oscillations in SLG (a) at $T = 1.3$ K and in BLG (b) at $T = 0.4$ K as a function of the carrier concentration for different total fields B_{tot} or tilt angles θ , respectively. When varying θ , the total field B_{tot} is adjusted such that the perpendicular field B_n remains constant, i.e., $B_{\text{tot}} = B_n / \cos \theta$. The oscillation maxima are marked with the corresponding Landau-level numbers N . The inset schematically shows this tilting configuration.

with cyclotron mass¹

$$m^* = \frac{\hbar^2}{2\pi} \left. \frac{dS(E)}{dE} \right|_{E=E_F} \quad (3)$$

and $A_0(N)$ is constant for a given N .

For the spherical Fermi surface in SLG and BLG with a Fermi wave vector $k_F = \sqrt{\pi n}$, the extremal cross section of the Landau orbits is $S(E)|_{E=E_F} = \pi k_F^2 = n\pi^2$, and Eq. (1) yields the concentration-dependent resistance oscillations as we observe them in our experiments:

$$\tilde{R}_{xx} = A \cos \left(\frac{\hbar\pi^2}{eB_n} n + \pi + \varphi_B \right) = A \cos \left(\frac{\pi}{2} \nu + \pi + \varphi_B \right), \quad (4)$$

where $\nu = (\hbar n)/(eB_n)$ is the filling factor. As expected, the oscillation period $(2eB_n)/(\hbar\pi)$ is independent on the band structure of the two-dimensional material and only depends on the filling factor.

To accurately determine the experimental oscillation amplitudes we have fitted our experimental data $R_{xx}(n)$ to Eq. (4) in two steps. First, we determined the oscillation period and a smooth background using all oscillations measured for a wide range of carrier concentrations. Second, we fitted the oscillation amplitudes A for each individual oscillation using the above determined period and background as fixed parameters. In Fig. 2 we show the final results of this fitting procedure for the SdH amplitude as a function of the total magnetic field for different Landau levels N . For clarity, all amplitudes are normalized to A_0 .

The experimentally observed reduction of the SdH amplitudes can be qualitatively visualized in a simple density of

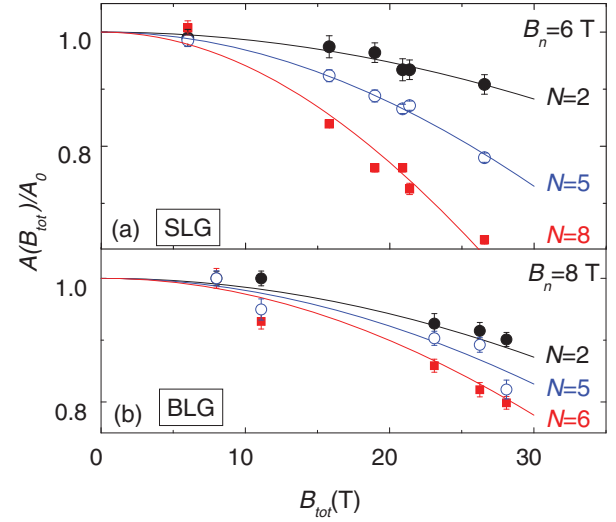


FIG. 2. (Color online) Normalized oscillation amplitudes as a function of total field B_{tot} at a constant perpendicular field B_n in SLG (a) and BLG (b). Error bars represent standard least-squares-fitting errors in the determination of A . Solid lines are fits to Eq. (2) with $m^* g^*$ as a fit parameter.

states (DOS) picture of a Landau level as depicted in Fig. 3(a). In a purely perpendicular magnetic field the Landau-level width exceeds the spin splitting and the DOS of the spin-down state [orange, horizontally dashed in Fig. 3(a)] overlaps with the one of the spin-up states (red, vertically dashed) to one broad Landau level. When increasing B_{tot} by leaving B_n constant, these two states move apart, yielding an additional broadening of the Landau level with a reduced DOS in the center [green, solid areas in Fig. 3(a)]. Eventually, when the spin splitting exceeds the level width, a minimum between two distinct levels starts to develop in the DOS. This scenario is indeed observed experimentally in SLG [Fig. 3(b)]. The SdH maxima corresponding to the $N = 9$ and $N = 10$ Landau levels at $B_{\text{tot}} = B_n = 5$ T do not show any splitting. Increasing

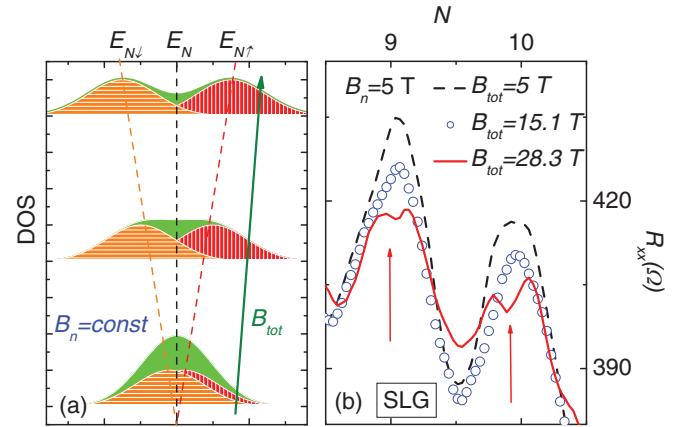


FIG. 3. (Color online) Schematic representation of the density of states for a Landau level with an increasing total magnetic field B_{tot} (from the bottom to the top) at a constant perpendicular component B_n (a). (b) shows this scenario as measured experimentally for the $N = 9, 10$ maximum in SLG at a constant perpendicular magnetic field $B_n = 5$ T.

the total field at a constant perpendicular component leads to a reduction of the oscillation amplitude and eventually to the appearance of spin-resolved peaks at the highest field of 28 T. However, this splitting is not yet enough to determine the energy difference by, e.g., activation measurements.

A quantitative analysis of this decrease of the SdH amplitudes with increasing total magnetic field is done by fitting the data to Eq. (2) with m^*g^* as a fitting parameter (solid lines in Fig. 2). The values for m^*g^* obtained are plotted as a function of the charge-carrier concentration in Fig. 4 for SLG (a) and BLG (b).

For both SLG and BLG the product m^*g^* increases with concentration, which can be mainly attributed to the concentration-dependent cyclotron mass m^* of particles with a linear¹ and hyperbolic dispersion¹⁵ as predicted by Eq. (3).

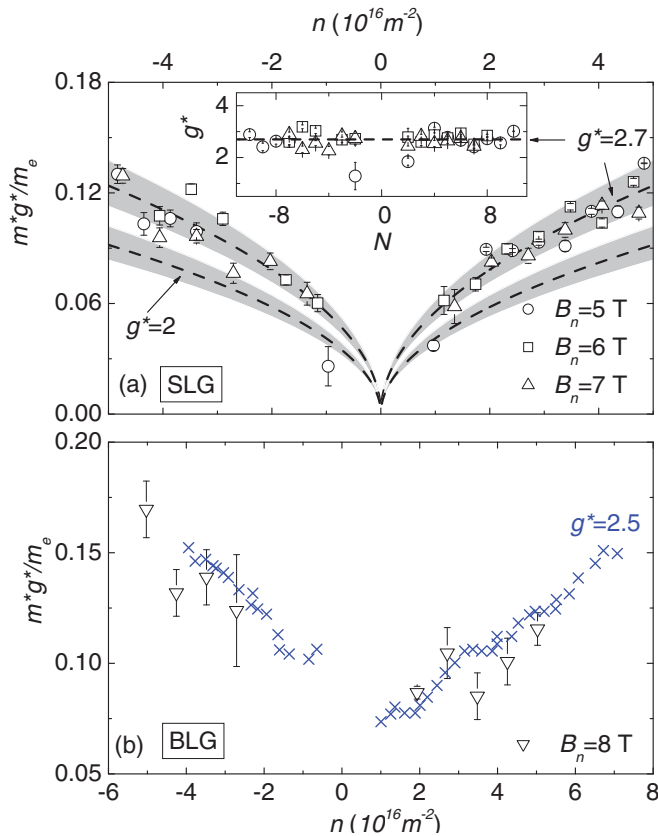


FIG. 4. (Color online) Experimentally deduced m^*g^* (open symbols), normalized to the free-electron mass m_e , as a function of charge-carrier concentration for SLG (a) and BLG (b). The individual data points were extracted from the total-field dependence of the SdH amplitudes corresponding to different Landau levels $N = 2, \dots, 10$ and represent measurements for a constant magnetic field $B_n = 5, 6$, and 7 T for SLG and $B_n = 8$ T for BLG. The error bars represent the standard least-squares-fitting errors, taking into account the error bars of A (Fig. 2). The dashed lines in (a) represent the calculated behavior of m^*g^* for different values of g^* , taking into account a 10% experimental uncertainty (shaded areas). The crosses in (b) compare our data to the experimental cyclotron mass for BLG (Ref. 17) multiplied by $g^* = 2.5$. The inset shows the effective g factor, extracted from the product m^*g^* in the main panel and the known cyclotron mass m^* in SLG, as a function of Landau-level index N .

The dashed lines in Fig. 4(a) show the calculated dependence of m^*g^* for $g^* = 2$ and $g^* = 2.7$ using $m^*(n) = (\hbar/c) \sqrt{\pi n}$.¹ The shadowed areas represent a 10% uncertainty of this calculation, mainly due to the experimental errors and some uncertainty in the Fermi velocity.¹⁶

For SLG [Fig. 4(a)], the increase of m^*g^* with n is symmetric for electrons and holes (i.e., negative and positive n in the figure). A best fit using $m^*(n)$ for SLG yields $g^* = 2.7 \pm 0.2$ (the error is the standard deviation). This finding is shown directly in the inset of Fig. 4(a), where we plot the value of g^* determined in the middle of each Landau level N for different perpendicular fields B_n . Within an experimental error g^* does not show any dependence on N or B_n .

For BLG [Fig. 4(b)] the experimental situation is more complex as the observed increase of m^*g^* with n is not symmetric for holes and electrons. Such a behavior is caused by an asymmetry of m^* resulting from an asymmetric band structure of biased BLG, which was already observed experimentally in transport experiments,¹⁷ cyclotron resonance,¹⁸ and activation-gap measurements.⁵ Applying the experimental cyclotron mass from Ref. 17 (depicted as crosses in Fig. 4) allows us to estimate g^* to be ~ 2.5 for both electrons and holes which is, within experimental accuracy, reasonably consistent with the g -factor enhancement observed in SLG.

The observed enhancement of the effective spin splitting compared to its free-electron value can be explained by an electron-electron interaction¹⁹ yielding an interaction-enhanced splitting between two spin levels within one Landau level:^{20,21}

$$g^* \mu_B B_{\text{tot}} = g \mu_B B_{\text{tot}} + E_{\text{ex}}^0 (n_{\downarrow} - n_{\uparrow}). \quad (5)$$

Here $g = 2$ is a free-electron g factor, E_{ex}^0 is an exchange parameter, and n_{\uparrow} and n_{\downarrow} are the relative occupations of the two spin states of a given Landau level.

For Gaussian-shaped Landau levels with broadening $\Gamma > g^* \mu_B B_{\text{tot}}$, i.e., where the spin splitting is not yet resolved, this relative occupation difference can be approximated by using the Taylor expansion of the Gauss error function $\text{erf}(g^* \mu_B B_{\text{tot}} / \Gamma)$:

$$n_{\downarrow} - n_{\uparrow} \approx \sqrt{\frac{1}{2\pi}} \frac{g^* \mu_B B_{\text{tot}}}{\Gamma}, \quad (6)$$

and Eq. (5) yields

$$\frac{g^*}{g} = \left(1 - \sqrt{\frac{1}{2\pi}} \frac{E_{\text{ex}}^0}{\Gamma} \right)^{-1}. \quad (7)$$

E_{ex}^0 is of the order of the Coulomb interaction $E_{\text{ex}}^0 \propto \sqrt{B_n}$,²¹ and $\Gamma \propto \sqrt{B_n}$.²² Therefore, the ratio E_{ex}^0 / Γ remains constant and the g -factor enhancement is indeed predicted to be constant, as we observe experimentally. Using the experimentally found $g^* = 2.7$ in Eq. (7) yields $E_{\text{ex}}^0 = 130$ K at 10 T when assuming $\Gamma = 200$ K.^{4,5} For a completely spin-polarized system, i.e., $n_{\downarrow} - n_{\uparrow} = 1$, one might then speculate that the exchange enhancement in Eq. (5) would be an order of magnitude larger than a single-particle Zeeman energy at this particular field.

Finally, we note that the experimentally found enhanced values of g^* in graphene are close to those observed in

transport experiments in graphite.²³ This may suggest that an exchange-induced enhancement of g^* is quite common for graphitic materials. In contrast, no interaction-induced g -factor enhancement is observed using electron-spin resonance in graphene²⁴ and graphite²⁵ since these measurements are not sensitive to many-body corrections.²⁶ Interestingly, measuring the Zeeman splitting of single-electron states in quantum dots, where no exchange enhancement of the g factor is expected, also yields $g \approx 2$,²⁷ albeit with a considerable experimental uncertainty.

To conclude, we have experimentally measured and analyzed spin splitting in SLG and BLG. We have shown that the product between the cyclotron mass m^* and the effective

g factor g^* increases with charge-carrier concentration, as expected for a linear dispersion in SLG and a hyperbolic dispersion in BLG. Using the known concentration dependence of m^* , we found that g^* in graphene is enhanced compared to the free-electron value, and we attribute this to electron-electron interaction effects.

Part of this work has been supported by EuroMagNETII under EU Contract No. 228043 and by the Stichting Fundamenteel Onderzoek der Materie (FOM), with financial support from the Nederlandse Organisatie voor Wetenschappelijk Onderzoek (NWO). The authors are grateful to Nacional de Grafite for supplying high-quality crystals of graphite.

*E.Kurganova@science.ru.nl

†U.Zeitler@science.ru.nl

¹K. S. Novoselov, A. K. Geim, S. V. Morozov, D. Jiang, M. I. Katsnelson, I. V. Grigorieva, S. V. Dubonos, and A. A. Firsov, *Nature (London)* **438**, 197 (2005).

²Y. Zhang, Y.-W. Tan, H. L. Stormer, and P. Kim, *Nature (London)* **438**, 201 (2005).

³K. S. Novoselov, E. McCann, S. V. Morozov, V. I. Fal'ko, M. I. Katsnelson, U. Zeitler, D. Jiang, F. Schedin, and A. K. Geim, *Nat. Phys.* **2**, 177 (2006).

⁴A. J. M. Giesbers, U. Zeitler, M. I. Katsnelson, L. A. Ponomarenko, T. M. Mohiuddin, and J. C. Maan, *Phys. Rev. Lett.* **99**, 206803 (2007).

⁵E. V. Kurganova, A. J. M. Giesbers, R. V. Gorbachev, A. K. Geim, K. S. Novoselov, J. C. Maan, and U. Zeitler, *Solid State Commun.* **150**, 2209 (2010).

⁶K. S. Novoselov, Z. Jiang, Y. Zhang, S. V. Morozov, H. L. Stormer, U. Zeitler, J. C. Maan, G. S. Boebinger, P. Kim, and A. K. Geim, *Science* **315**, 1379 (2007).

⁷A. J. M. Giesbers, L. A. Ponomarenko, K. S. Novoselov, A. K. Geim, M. I. Katsnelson, J. C. Maan, and U. Zeitler, *Phys. Rev. B* **80**, 201403 (2009).

⁸Z. Jiang, Y. Zhang, H. L. Stormer, and P. Kim, *Phys. Rev. Lett.* **99**, 106802 (2007).

⁹I. M. Lifshitz and A. M. Kosevich, *Zh. Eksp. Teor. Fiz.* **29**, 730 (1955) [*Sov. Phys. JETP* **2**, 636 (1956)].

¹⁰E. N. Adams and T. D. Holstein, *J. Phys. Chem. Solids* **10**, 254 (1959).

¹¹K. S. Novoselov, A. K. Geim, S. V. Morozov, D. Jiang, Y. Zhang, S. V. Dubonos, I. V. Grigorieva, and A. A. Firsov, *Science* **306**, 666 (2004).

¹²A. E. Stephens, D. G. Seiler, J. R. Sybert, and H. J. Mackey, *Phys. Rev. B* **11**, 4999 (1975).

¹³R. B. Dingle, *Proc. R. Soc. London, Ser. A* **211**, 500 (1952).

¹⁴F. F. Fang and P. J. Stiles, *Phys. Rev.* **174**, 823 (1968).

¹⁵E. McCann and V. I. Fal'ko, *Phys. Rev. Lett.* **96**, 086805 (2006).

¹⁶R. Gillen and J. Robertson, *Phys. Status Solidi B* **247**, 2945 (2010).

¹⁷E. V. Castro, K. S. Novoselov, S. V. Morozov, N. M. R. Peres, J. M. B. Lopes dos Santos, J. Nilsson, F. Guinea, A. K. Geim, and A. H. Castro Neto, *Phys. Rev. Lett.* **99**, 216802 (2007).

¹⁸E. A. Henriksen, Z. Jiang, L.-C. Tung, M. E. Schwartz, M. Takita, Y. J. Wang, P. Kim, and H. L. Stormer, *Phys. Rev. Lett.* **100**, 087403 (2008).

¹⁹T. Ando and Y. Uemura, *J. Phys. Soc. Jpn.* **37**, 1044 (1974).

²⁰T. Englert, D. Tsui, A. Gossard, and C. Uihlein, *Surf. Sci.* **113**, 295 (1982).

²¹R. J. Nicholas, R. J. Haug, K. v. Klitzing, and G. Weimann, *Phys. Rev. B* **37**, 1294 (1988).

²²T. Ando, A. B. Fowler, and F. Stern, *Rev. Mod. Phys.* **54**, 437 (1982).

²³J. M. Schneider, N. A. Goncharuk, P. Vasek, P. Svoboda, Z. Vyborny, L. Smrcka, M. Orlita, M. Potemski, and D. K. Maude, *Phys. Rev. B* **81**, 195204 (2010).

²⁴S. S. Rao, A. Stesmans, K. Keunen, D. V. Kosynkin, A. Higginbotham, and J. M. Tour, *Appl. Phys. Lett.* **98**, 083116 (2011).

²⁵K. Matsubara, T. Tsuzuku, and K. Sugihara, *Phys. Rev. B* **44**, 11845 (1991).

²⁶W. Kohn, *Phys. Rev.* **123**, 1242 (1961).

²⁷J. Guttinger, T. Frey, C. Stampfer, T. Ihn, and K. Ensslin, *Phys. Rev. Lett.* **105**, 116801 (2010).